

A Field-directional Specific Heat Study on the Gap Structure of Overdoped $\text{Ba}(\text{Fe}_{1-x}\text{Co}_x)_2\text{As}_2$

Gang Mu^{1,5*}, Jun Tang², Yoichi Tanabe², Jingtao Xu², Bin Zeng³, Bing Shen³, Fei Han³,
Hai-Hu Wen^{3,4}, Satoshi Heguri¹ and Katsumi Tanigaki^{1,2†}

¹*Department of Physics, Graduate School of Science, Tohoku University, Sendai 980-8578, Japan*

²*WPI-AIMR, Tohoku University, Sendai 980-8578, Japan*

³*Institute of Physics and Beijing National Laboratory for Condensed Matter Physics, Chinese Academy of Sciences, Beijing 100190, China*

⁴*National Laboratory for Solid State Microstructures, Department of Physics, Nanjing University, Nanjing 210093, China*

⁵*State Key Laboratory of Functional Materials for Informatics, Shanghai Institute of Microsystem and Information Technology, Chinese Academy of Sciences, Shanghai 200050, China*

Low-temperature specific heat is measured on the overdoped $\text{Ba}(\text{Fe}_{1-x}\text{Co}_x)_2\text{As}_2$ ($x = 0.13$) single crystal under magnetic fields along three different directions. A clear anisotropy is observed on the field dependent electronic specific heat coefficient $\gamma(H)$. The value of $\gamma(H)$ is obviously larger with magnetic field along [001] (c -axis) than that within the ab -plane of the crystal lattice, which cannot be attributed to the effect by anisotropy of the upper critical field. Meanwhile, the data show a rather small difference when the direction of the field is rotated from [100] to [110] direction within the ab -plane. Our results suggest that a considerable part of the line nodes is not excited to contribute to the quasiparticle density of states by the field when the field is within the ab -plane. The constraints on the topology of the gap nodes are discussed based on our observations.

KEYWORDS: Fe-based superconductors, gap structure, specific heat, $\text{Ba}(\text{Fe}_{1-x}\text{Co}_x)_2\text{As}_2$, line nodes

1. Introduction

Knowledge of the gap structure will supply very important information for the understanding of the superconducting pairing mechanism, which is a central issue in the physics of

*E-mail: mugang@sspns.phys.tohoku.ac.jp

†E-mail: tanigaki@sspns.phys.tohoku.ac.jp

unconventional superconductors. Up to date, gap structure of the Fe-based superconductors seems to be more complicated than expected, which is found to vary substantially from family to family. The consensus has been reached on several systems, e.g. LaFePO,^{1,2)} LiFeP,³⁾ KFe₂As₂,^{4,5)} BaFe₂(As_{1-x}P_x)₂,⁶⁻⁸⁾ and so on, that nodes exist on the gap structure. And node-less superconductivity seems to have been confirmed in the K_xFe_{2-y}Se₂ system⁹⁻¹²⁾ on the other hand. However, experimental results gave rather contradicting conclusions on this issue in other systems of the Fe-based superconductors.¹³⁻²⁵⁾ Furthermore, recent experiments reveal that the gap structure can modulate with the doping concentration even in the same family. In the case of electron-doped (Co- or Ni- doped) 122 system, the increase in the gap anisotropy and even the emergence of gap nodes, as the doping content increases in the overdoped region, are evidenced by many experimental methods.^{23,24,26-29)} This behavior is attributed to the enhancement of intraband interaction and pair scattering between the electron-like Fermi surfaces as the system is doped away from the optimal point.³⁰⁾ Many efforts have been made to obtain more information about the location and direction of the nodes. Directional penetration depth measurements have suggested latitudinal circular line nodes located at the finite k_z wave vector or a point (or extended area) polar node.²³⁾ Based on the directional heat transport measurements, a simplified two-band model of the Fermi surface (FS) was proposed, where line nodes on one FS sheet with strong 3D character and a deep minimum of the gap on the other FS sheet with quasi-2D character are suggested.²⁴⁾ A theoretical analysis has shown that the line nodes may form vertical loops in the presence of hybridization between two electron pockets.³¹⁾ For the BaFe₂(As_{0.7}P_{0.3})₂ system, angle-resolved thermal conductivity measurements have suggested the closed nodal loops at the flat parts of the electron FS.⁷⁾ In contrast, an angle resolved photoemission spectroscopy (ARPES) study has revealed a horizontal circular line node on the hole FS around the Z point at the Brillouin zone boundary.⁸⁾

Specific heat (SH) is a powerful bulk probe for investigating the gap structure of the unconventional superconductors. The variation of electronic SH (C_{el}) versus temperature (T) strongly depends on the gap structures of the superconducting materials.^{32,33)} In our previous studies,²⁷⁾ we have observed a clear T^2 term in C_{el} of the overdoped Ba(Fe_{1-x}Co_x)₂As₂, giving a direct evidence for the presence of line nodes in the energy gap, in sharp contrast to that observed in the underdoped and optimal doped samples which show a rather small anisotropy in the energy gap. In the mixed state, the applied field (H) can induce vortices with a supercurrent flowing perpendicularly to H . The low-energy quasiparticles will undergo a Doppler shift induced by the supercurrent, which can give rise to a considerable enhancement of C_{el}

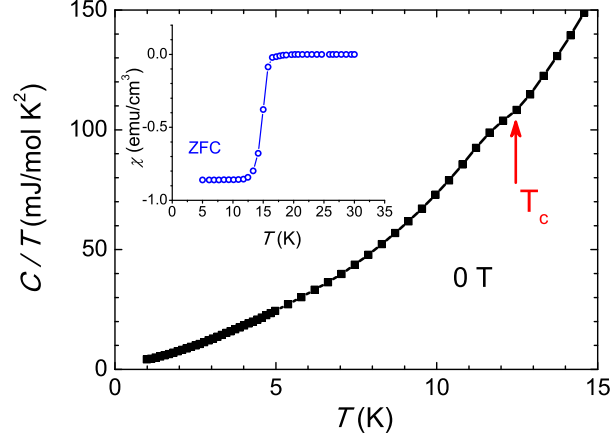


Fig. 1. (Color online) Main frame: temperature dependence of SH coefficient (C/T) for the overdoped $\text{Ba}(\text{Fe}_{1-x}\text{Co}_x)_2\text{As}_2$ with $x = 0.13$ under zero field. The red arrow denotes the specific heat anomaly due to the superconducting transition. Inset: dc susceptibility for the same sample measured using the zero-field-cooling process. The dc field of 10 Oe was applied perpendicular to the c -axis.

for a nodal superconductor.^{34,35} This is called the Volovik effect. Doppler-shift energy is determined by $\delta E \propto \vec{v}_s \cdot \vec{v}_F$, where \vec{v}_s and \vec{v}_F are the supercurrent velocity and Fermi velocity respectively. We note that v_F is proportional to $\nabla_k E(k)$ and thus it is perpendicular to the Fermi surface. Moreover, Volovik effect works mainly at the places near the nodes. So the Volovik effect is the strongest (weakest) when H is parallel (perpendicular) to the Fermi surface where the nodes reside. This provides valuable information on the topology of the line nodes, when we compare the SH data obtained with H along different directions of the crystal lattice.

In order to obtain further information on the topology of the line nodes, here we report a field-directional specific heat study on the overdoped $\text{Ba}(\text{Fe}_{1-x}\text{Co}_x)_2\text{As}_2$. The unambiguous anisotropic behaviors related to the Volovik effect imposed on line nodes are confirmed by the fact that the electronic SH coefficient $\gamma(H)$ increases more quickly when the field is parallel to the c -axis than that within the ab -plane. The possible constraints on the topology of line nodes are discussed based on our observations.

2. Experimental Details and Sample Characterization

The $\text{Ba}(\text{Fe}_{1-x}\text{Co}_x)_2\text{As}_2$ single crystals were grown by a self-flux method using FeAs as the flux. As-grown samples were annealed under high vacuum at 800 °C for 20 days. An identical crystal is used for all the measurements in this paper, which has a dimensions of

about $2.4 \times 2.0 \times 0.2 \text{ mm}^3$ and the mass of about 6.5 mg. The dc magnetization measurements were made with a superconducting quantum interference device (Quantum Design, MPMS). Specific heat was measured with magnetic field along three directions (see figure 2(a)) in the field-cooling mode. The data obtained with H within ab -plane were collected with a Helium-3 system attached with the physical property measurement system (Quantum Design, PPMS), while those with H along c -axis were obtained from PPMS. We employed the thermal relaxation technique to perform the specific heat measurements. The thermometer has been calibrated under different magnetic fields beforehand.

The superconducting transition of the selected sample with nominal doping contents $x = 0.13$ is checked by the dc magnetization and specific heat measurements. The present sample was determined to be in the overdoped region of the phase diagram.²⁷⁾ It has been confirmed by many measurements that no magnetic order exists in this doping region.^{36,37)} So it supplies a very clean platform to study the behaviors of specific heat. In figure 1, we show the temperature dependence of the SH coefficient C/T up to 15 K under zero field. The kink at about 12.5 K indicated by red arrow is the superconducting transition. This temperature corresponds to the end point of the diamagnetic transition, as shown in the inset of figure 1. The superconducting volume fraction estimated from the magnitude of the dc susceptibility suggests a nearly full Meissner fraction for the present sample.

3. Results

We measured SH of $\text{Ba}(\text{Fe}_{1-x}\text{Co}_x)_2\text{As}_2$ with $x = 0.13$ under field along the [100], [110], and [001] directions of the crystal lattice. A schematic representation of the three directions is given in figure 2(a). The raw data of SH under H of these three directions are plotted as C/T vs T^2 in figures 2(b)-(d), respectively. Here we focus on the behaviors of our data in the low- T region below 4.5 K. One can see that the behaviors of the data with H along [100] and [110] directions are quite similar with each other. While the data with H along the [001] direction increase more quickly with H . Nevertheless, all the three sets of data show clear negative curvatures in the temperature range we studied. In our previous work,²⁷⁾ we have attributed this behavior to the presence of the T^2 term in the electronic SH, which is consistent with the prediction for the superconductors with line nodes in the energy gap. No Schottky anomaly can be seen in our data suggesting a very low concentration of the magnetic impurity in our sample. The data were then fitted by the following equation

$$C(T, H) = \gamma(H)T + \alpha(H)T^2 + \beta T^3, \quad (1)$$

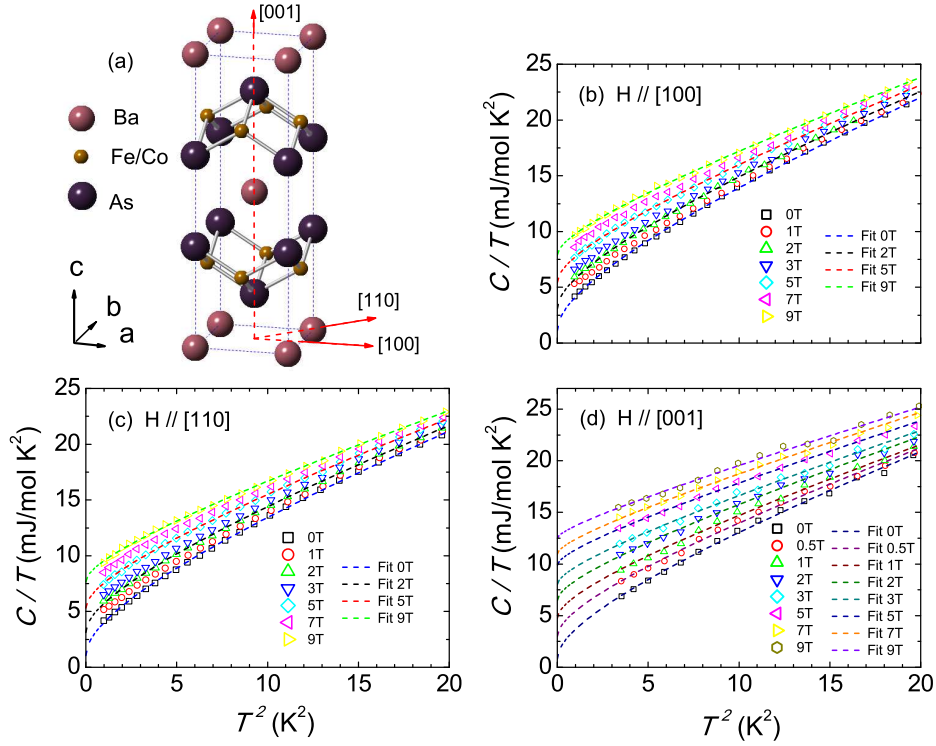


Fig. 2. (Color online) (a) Crystal structure of $\text{Ba}(\text{Fe}_{1-x}\text{Co}_x)_2\text{As}_2$. Red arrowed lines represent the three directions of the crystal lattice along which the magnetic field is applied. (b)-(d) show the raw data of the SH for the sample with $x = 0.13$ under fields aligned with the [100], [110], and [001] directions of the crystal lattice, respectively. The dashed lines represent the results of theoretical fitting (see text).

where $\gamma(H)$ is the electronic SH coefficient under H , $\alpha(H)$ is the coefficient of the T^2 term under H , and β is the phonon SH coefficient. The value of β was found to be almost independent of the field, with deviation below the scale of 5%. Consequently, here we average the value of β under different fields and fix it when fitting the data using equation (1). The effect of small fluctuations of β is transferred to the error bar of the resulting fitting parameters $\gamma(H)$ and $\alpha(H)$ (see figure 3). The fitting results are displayed by the dashed lines in figure 2. Only four selected fitting curves are shown in figures 2(b) and (c) respectively for clarity. It is clear that these curves describe the negative-curvature features commendably. From the fitting we find that the residual electronic SH coefficient $\gamma(H = 0)$ for the three sets of data shows very close value of about 1 mJ/mol K^2 . This value is smaller than the previously reported results in the similar systems,^{26,38)} suggesting the high quality of our sample.

We note here multi-gap effect should be considered when fitting our data in principle in such a multi-band system, because the magnitude and structure of the gaps on different FS sheets may be rather different. However, one difficulty is that the number of the parameters

will be too many to give a reliable fitting, if we take all the five bands into account simultaneously. Fortunately, the electronic SH is mainly contributed from the quasiparticles with heavy mass, which have been found to come from hole pockets by band calculations. So our observations imply that line nodes may exist on one of the hole pockets. Moreover, electronic SH from the pockets with line nodes will overcome that from fully gapped pockets in the low temperature limit, because the latter should follow an exponential law with temperature. Consequently, it is safe to neglect the contributions from other fully gapped pockets when fitting the low-temperature data. For the same reason, we will only consider the FS sheet with line nodes when discussing the possible topologies of the gap nodes in the next section.

The fitting parameters $\gamma(H)$ and $\alpha(H)$ are shown in figures 3(a) and (b). The x -coordinate is normalized with the upper critical field H_{c2} , so as to eliminate the effect of anisotropy of H_{c2} on the H dependent data. As we have stated,²⁷⁾ H_{c2} within the ab -plane is about 28 T, from which the H_{c2} value along the c -axis can be estimated using the its anisotropy ($\Gamma \equiv H_{c2}^{ab}/H_{c2}^c$). From the reported high- H experiments, we know that Γ decreases when reducing T and finally reaches about 1.1 at 0.7 K for the near-optimal doped $\text{Ba}(\text{Fe}_{1-x}\text{Co}_x)_2\text{As}_2$.^{39,40)} Here we take the value $\Gamma \sim 1.3$ for the present overdoped case, which would be no less than the actual value. Such a treatment will not affect the conclusions described below, because a smaller Γ would result in the enhancement of the anisotropic features.

Both $\gamma(H)$ and $\alpha(H)$ show small deviations among the three directions when H is approaching zero, which confirms the reliability of our data even though the data with H along c -axis is only measured down to 1.9 K. From figure 3(a) one can see that all the three sets of data are clearly above the blue dashed line, which represents the theoretical curve for the case with an isotropic gap. This is consistent with the features induced by the Volovik effect in a nodal superconductor. It is clear that $\gamma(H)$ with H aligned with c -axis (hereafter abbreviated as $\gamma^c(H)$) increases more quickly than that within the ab -plane (abbreviated as $\gamma^{ab}(H)$). We found that $\gamma^{ab}(H)$ takes up about 70% of $\gamma^c(H)$ when the reduced H/H_{c2} equals to 0.3. In sharp contrast, the data within the ab -plane remain almost unchanged within the extent of error bar when H is rotated from [100] to [110] direction. Considering the fact that the increase of $\gamma(H)$ is induced by Volovik effect, our present observations suggest that the Volovik effect is stronger when H is applied along the c -axis than that within the ab -plane. The anisotropic features of H dependent $\alpha(H)$ shown in figure 3(b) also support such an argument because the decrease of $\alpha(H)$ is associated with the Volovik effect. The T^2 term reflects the V-shape of the density of states (DOS) at the nodes.³³⁾ And the Volovik effect induced by magnetic field will destroy the V-shape of DOS in the low-energy limit. We note that our argument here

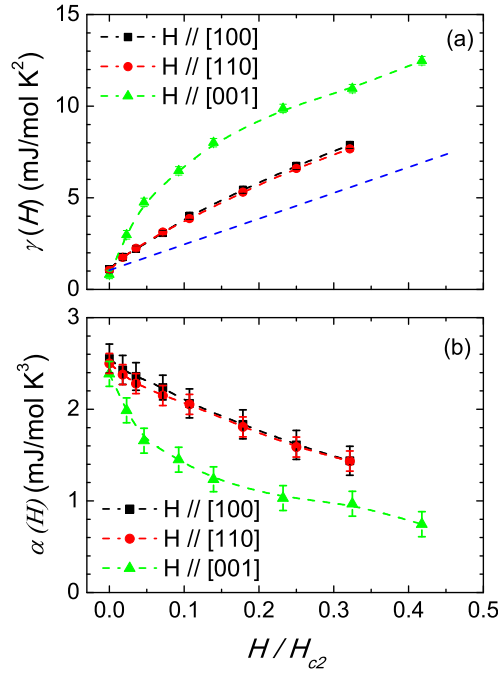


Fig. 3. (Color online) Field dependence of $\gamma(H)$ and $\alpha(H)$ with H along three directions. H is normalized with the upper critical field H_{c2} . The blue dashed line in (a) shows the theoretical curve for the case with an isotropic gap. Other dashed lines are guides to the eye.

is different from previously reported field-directional SH data on similar systems, where the anisotropic behaviors of $\gamma(H)$ were only attributed to the effect of anisotropy of H_{c2} ³⁸⁾ which would result in an overestimation of Γ (> 2). Obviously, the findings here will provide a hint for investigating the topology of the nodes, which will be discussed in the next section.

4. Discussion

As we have stated, different topologies of the nodes or gap minima have been proposed from different measurements and calculations. Generally speaking, three typical models can be anticipated, namely vertical line nodes, horizontal line nodes and vertical loop nodes. Also the significant influence by the three-dimensional (3D) features of the Fermi surface (FS) has been noticed by band-calculations.^{41,42)} Consequently, here we consider the constraints by our data on the line nodes based on the two simple models, where vertical and horizontal line nodes are located on one of the FSs with a certain extent of 3D character. The situation of vertical loop nodes can be considered as a mixture of the case of the simple vertical and horizontal line nodes, in principle. As shown in figure 4, the longitudinal section of the FS sheet is shown by two black lines. The red line in figure 4(a) and red circle in figure 4(b)

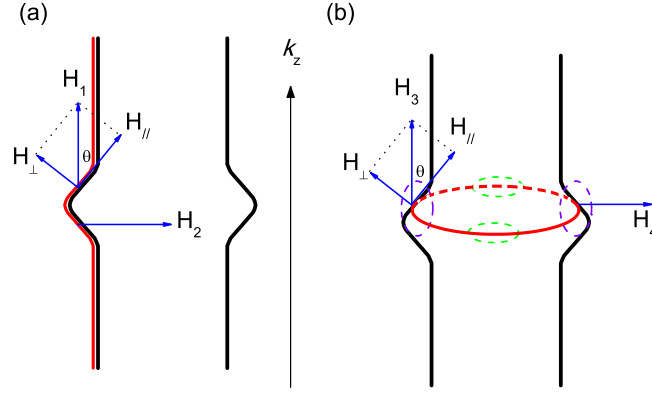


Fig. 4. (Color online) Schematic diagram of two typical models of line nodes on one of the Fermi surfaces with a 3D character. Here we only display a longitudinal section of the Fermi surface shown by the two black lines. The vertical (a) and horizontal (b) line nodes are shown by the red lines.

represent the positions of vertical and horizontal line nodes, respectively. The anisotropy of Fermi velocity and other details of the Fermi surfaces are not taken into account in the present simple models. Considering the fact that the hole pockets have heavier mass quasiparticles than the electron pockets, most of the electronic SH is contributed from the hole FS sheets. So the FS sheets shown in figure 4 should most likely be one of the hole FS sheets around the Γ point.

We first check the situation of the vertical-node case as shown in figure 4(a). When H is applied parallel to k_z , which is shown by the blue arrow H_1 , the segments of line nodes on the FS with no or small 3D features will experience a strong Volovik effect, while that with clear 3D features only undergo a depressed Volovik effect induced by the projection of H on the tangent surface ($H_{\parallel} = H_1 \cos \theta$), where angle θ describes the deviation of the FS from the direction of k_z . When H is perpendicular to k_z , the situation will be rather complex because the direction can be rotated by 360° . The Volovik effect is the weakest if H is rotated to the nodal direction (see H_2 in figure 4(a)) because only the segments of nodes on the 3D-dispersed FS can experience the Volovik effect with a projected field $H_{\parallel} = H_2 \sin \theta$. The situations with H along other directions may vary depending on the number of the vertical line nodes and their distribution on the FS. Nevertheless, the clear anisotropy between $\gamma^c(H)$ and $\gamma^{ab}(H)$ requires that the angle θ or the proportion of the 3D-dispersed FS should not be too large.

One problem in the scenario described above is that $\gamma^{ab}(H)$ should show some variation in principle when H is rotated within ab -plane, which was not observed in our data. One

possibility is that the number of nodes is large (e.g. larger than 4). In this case, the angle dependent behavior of $\gamma^{ab}(H)$ will be un conspicuous and difficult to be detected from the measurements. Another explanation may be given by calculations based on an extended-s-wave case,⁴³⁾ where an attenuation of the SH vibration is predicted because of the elliptical FS pockets near the M points. It seems that both cases do not support the *d*-wave symmetry of the energy gap. At present we can't rule out the possibility that both [100] and [110] directions deviate from the nodal direction, and consequently we failed to observe the difference between the two directions. This may need further clarification by detailed angle-resolved SH measurements.

The situation becomes somewhat different if we have the horizontal line nodes, as shown in figure 4(b). When H is parallel to k_z (see H_3), the whole nodal line will experience a depressed Volovik effect induced by $H_{\parallel} = H_3 \cos \theta$. Whereas when H is applied perpendicular to k_z (see H_4), the segments of nodes on the areas of the FS marked by the green circles will experience a strong Volovik effect because H is roughly parallel to these parts of FS. Meanwhile, the segments of nodes marked by the violet circles will experience a depressed Volovik effect induced by $H_{\parallel} = H_4 \sin \theta$. The fact that $\gamma^c(H)$ is clearly larger than $\gamma^{ab}(H)$ in our data means that the overall Volovik effect when H is parallel to k_z should exceed that with H perpendicular to k_z . This implies that the angle θ cannot be too large. The advantage of this model is that the unobservable vibration of $\gamma^{ab}(H)$ can be explained naturally. We note that this horizontal-line-nodes model is rather similar to that observed in $\text{BaFe}_2(\text{As}_{0.7}\text{P}_{0.3})_2$ by the ARPES measurements.⁸⁾

5. Concluding remarks

In summary, we studied the low-temperature SH on the overdoped $\text{Ba}(\text{Fe}_{1-x}\text{Co}_x)_2\text{As}_2$ with magnetic field along three different directions. Clear anisotropic behaviors are observed from H dependent data. The electronic SH coefficient $\gamma(H)$ increases more quickly when H is in the *c*-axis direction than that within the *ab*-plane, whereas the data remain unchanged within our resolution when H is rotated within the *ab*-plane. Our results suggest that a considerable portion of the line nodes is not excited completely to contribute to the density of states when H is in the *ab* in-plane. These conclusions supply important constraints when investigating the topologies of the line nodes in this system.

Acknowledgment

We acknowledge discussions with Dr. Yue Wang. The research is partially supported by Scientific Research on Priority Areas of New Materials Science Using Regulated Nano Spaces, the Ministry of Education, Science, Sports and Culture, Grant-in-Aid for Science, and Technology of Japan. The work is partially supported by Tohoku GCOE Program and by the approval of the Japan Synchrotron Radiation Research Institute (JASRI). This work is partially supported by the Knowledge Innovation Project of Chinese Academy of Sciences (No. KJCX2-EW-W11). G M expresses special thanks to Grants-in-Aid for Scientific Research from the Japan Society for the Promotion of Science (JSPS) (Grant No. P10026).

References

- 1) J. D. Fletcher, A. Serafin, L. Malone, J. G. Analytis, J. H. Chu, A. S. Erickson, I. R. Fisher, and A. Carrington: Phys. Rev. Lett. **102** (2009) 147001.
- 2) C. W. Hicks, T. M. Lippman, M. E. Huber, J. G. Analytis, J. H. Chu, A. S. Erickson, I. R. Fisher, and K. A. Moler: Phys. Rev. Lett. **103** (2009) 127003.
- 3) K. Hashimoto, S. Kasahara, R. Katsumata, Y. Mizukami, M. Yamashita, H. Ikeda, T. Terashima, A. Carrington, Y. Matsuda, and T. Shibauchi: Phys. Rev. Lett. **108** (2012) 047003.
- 4) J. K. Dong, S. Y. Zhou, T. Y. Guan, H. Zhang, Y. F. Dai, X. Qiu, X. F. Wang, Y. He, X. H. Chen, and S. Y. Li: Phys. Rev. Lett. **104** (2010) 087005.
- 5) H. Fukazawa, Y. Yamada, K. Kondo, T. Saito, Y. Kohori, K. Kuga, Y. Matsumoto, S. Nakatsuji, H. Kito, P. M. Shirage, K. Kihou, N. Takeshita, C. H. Lee, A. Iyo, and H. Eisaki: J. Phys. Soc. Jpn. **78** (2009) 083712.
- 6) K. Hashimoto, M. Yamashita, S. Kasahara, Y. Senshu, N. Nakata, S. Tonegawa, K. Ikada, A. Serafin, A. Carrington, T. Terashima, H. Ikeda, T. Shibauchi, and Y. Matsuda: Phys. Rev. B **81** (2010) 220501(R).
- 7) M. Yamashita, Y. Senshu, T. Shibauchi, S. Kasahara, K. Hashimoto, D. Watanabe, H. Ikeda, T. Terashima, I. Vekhter, A. B. Vorontsov, and Y. Matsuda: Phys. Rev. B **84** (2011) 060507.
- 8) Y. Zhang, Z. R. Ye, Q. Q. Ge, F. Chen, J. Jiang, M. Xu, B. P. Xie, and D. L. Feng: Nature Physics **8** (2012) 371.
- 9) D. X. Mou, S. Y. Liu, X. W. Jia, J. F. He, Y. Y. Peng, L. Zhao, L. Yu, G. D. Liu, S. L. He, X. L. Dong, J. Zhang, H. D. Wang, C. H. Dong, M. H. Fang, X. Y. Wang, Q. J. Peng, Z. M. Wang, S. J. Zhang, F. Yang, Z. Y. Xu, C. T. Chen, and X. J. Zhou: Phys. Rev. Lett. **106** (2011) 107001.
- 10) X. P. Wang, T. Qian, P. Richard, P. Zhang, J. Dong, H. D. Wang, C. H. Dong, M. H. Fang, and H. Ding: Europhys. Lett. **93** (2011) 57001.
- 11) B. Zeng, B. Shen, G. F. Chen, J. B. He, D. M. Wang, C. H. Li, and H. H. Wen: Phys. Rev. B **83** (2011) 144511.
- 12) L. Zhao, D. X. Mou, S. Y. Liu, X. W. Jia, J. F. He, Y. Y. Peng, L. Yu, G. D. Liu, S. L. He, X. L. Dong, J. Zhang, J. B. He, D. M. Wang, G. F. Chen, J. G. Guo, X. Y. Wang, Q. J.

- Peng, Z. M. Wang, S. J. Zhang, F. Yang, Z. Y. Xu, C. T. Chen, and X. J. Zhou: Phys. Rev. B **83** (2011) 140508(R).
- 13) G. Mu, X. Zhu, L. Fang, L. Shan, C. Ren, and H. H. Wen: Chin. Phys. Lett. **25** (2008) 2221.
 - 14) T. Y. Chen, Z. Tesanovic, R. H. Liu, X. H. Chen, and C. L. Chien: Nature (London) **453** (2008) 1224.
 - 15) H. Ding, P. Richard, K. Nakayama, K. Sugawara, T. Arakane, Y. Sekiba, A. Takayama, S. Souma, T. Sato, T. Takahashi, Z. Wang, X. Dai, Z. Fang, G. F. Chen, J. L. Luo, and N. L. Wang: Europhys. Lett. **83** (2008) 47001.
 - 16) K. Hashimoto, T. Shibauchi, T. Kato, K. Ikada, R. Okazaki, H. Shishido, M. Ishikado, H. Kito, A. Iyo, H. Eisaki, S. Shamoto, and Y. Matsuda: Phys. Rev. Lett. **102** (2009) 017002.
 - 17) C. Ren, Z. S. Wang, H. Q. Luo, H. Yang, L. Shan, and H. H. Wen: Phys. Rev. Lett. **101** (2008) 257006.
 - 18) G. Mu, H. Q. Luo, Z. S. Wang, L. Shan, C. Ren, and H. H. Wen: Phys. Rev. B **79** (2009) 174501.
 - 19) J. P. Reid, M. A. Tanatar, X. G. Luo, H. Shakeripour, S. R. de Cotret, N. D. Leyraud, J. Chang, B. Shen, H.-H. Wen, H. Kim, R. Prozorov, L. Taillefer: arXiv: 1105.2232.
 - 20) B. Zeng, G. Mu, H. Q. Luo, T. Xiang, I. I. Mazin, H. Yang, L. Shan, C. Ren, P. C. Dai, and H. H. Wen: Nat. Commun. **1** (2010) 112.
 - 21) H. Miao, P. Richard, Y. Tanaka, K. Nakayama, T. Qian, K. Umezawa, T. Sato, Y.-M. Xu, Y.-B. Shi, N. Xu, X.-P. Wang, P. Zhang, H.-B. Yang, Z.-J. Xu, J. S. Wen, G.-D. Gu, X. Dai, J.-P. Hu, T. Takahashi, and H. Ding: Phys. Rev. B **85** (2012) 094506.
 - 22) C. L. Song, Y. L. Wang, P. Cheng, Y. P. Jiang, W. Li, T. Zhang, Z. Li, K. He, L. L. Wang, J. F. Jia, H. H. Hung, C. J. Wu, X. C. Ma, X. Chen, and Q. K. Xue: Science **332** (2011) 1410.
 - 23) C. Martin, H. Kim, R. T. Gordon, N. Ni, V. G. Kogan, S. L. Budko, P. C. Canfield, M. A. Tanatar, and R. Prozorov, Phys. Rev. B **81**, 060505(R) (2010).
 - 24) J. P. Reid, M. A. Tanatar, X. G. Luo, H. Shakeripour, N. Doiron-Leyraud, N. Ni, S. L. Bud'ko, P. C. Canfield, R. Prozorov, and L. Taillefer: Phys. Rev. B **82** (2010) 064501.
 - 25) B. Zeng, G. Mu, B. Shen, P. Cheng, H. Luo, H. Yang, L. Shan, C. Ren, and H. H. Wen: Phys. Rev. B **85** (2012) 224514.

- 26) K. Gofryk, A. B. Vorontsov, I. Vekhter, A. S. Sefat, T. Imai, E. D. Bauer, J. D. Thompson, and F. Ronning: Phys. Rev. B **83** (2011) 064513.
- 27) G. Mu, J. Tang, Y. Tanabe, J. T. Xu, S. Heguri, and K. Tanigaki: Phys. Rev. B **84** (2011) 054505.
- 28) C. Ren, Z. S. Wang, Z. Y. Wang, H. Q. Luo, X. Y. Lu, B. Sheng, C. H. Li, L. Shan, H. Yang, and H. H. Wen: e-print arXiv:1106.2891.
- 29) T. Fischer, A. V. Pronin, J. Wosnitza, K. Iida, F. Kurth, S. Haindl, L. Schultz, B. Holzapfel, and E. Schachinger: Phys. Rev. B **82** (2010) 224507.
- 30) P. J. Hirschfeld, M. M. Korshunov, and I. I. Mazin: Rep. Prog. Phys. **74** (2011) 124508.
- 31) M. Khodas, and A. V. Chubukov: Phys. Rev. B **86** (2012) 144519.
- 32) M. Sigrist and K. Ueda: Rev. Mod. Phys. **63** (1991) 239.
- 33) N. E. Hussey: Advances in Physics, **51** (2002) 1685.
- 34) G. E. Volovik: JETP Lett. **58** (1993) 469.
- 35) G. E. Volovik: JETP Lett. **65** (1997) 491.
- 36) J. H. Chu, J. G. Analytis, C. Kucharczyk, and I. R. Fisher: Phys. Rev. B (2009) **79** 014506.
- 37) C. Lester, J. H. Chu, J. G. Analytis, S. Capelli, A. S. Erickson, C. L. Condon, M. F. Toney, I. R. Fisher, and S. M. Hayden: Phys. Rev. B **79** (2009) 144523.
- 38) D. J. Jang, A. B. Vorontsov, I. Vekhter, K. Gofryk, Z. Yang, S. Ju, J. B. Hong, J. H. Han, Y. S. Kwon, F. Ronning, J. D. Thompson, and T. Park: New J. Phys. **13** (2011) 023036.
- 39) M. Kano, Y. Kohama, D. Graf, F. Balakirev, A. S. Sefat, M. A. McGuire, B. C. Sales, D. Mandrus, and S. W. Tozer: J. Phys. Soc. Jpn. **78** (2009) 084719.
- 40) A. Yamamoto, J. Jaroszynski, C. Tarantini, L. Balicas, J. Jiang, A. Gurevich, D. C. Larbalestier, R. Jin, A. S. Sefat, M. A. McGuire, B. C. Sales, D. K. Christen, and D. Mandrus: Appl. Phys. Lett. **94** (2009) 062511.
- 41) S. Graser, A. F. Kemper, T. A. Maier, H.-P. Cheng, P. J. Hirschfeld, and D. J. Scalapino: Phys. Rev. B **81** (2010) 214503.
- 42) K. Suzuki, H. Usui, and K. Kuroki: J. Phys. Soc. Jpn. **80** (2011) 013710.
- 43) S. Graser, G. R. Boyd, C. Cao, H. P. Cheng, P. J. Hirschfeld, and D.J. Scalapino: Phys. Rev. B **77** (2008) 180514(R).